S1 Context

This supplement aims to answer the following comment :

"Since the transports Q, Q_{Eu} and Q_r (and other quantitative estimates) are based on measurements which contain random error, it is important to have error bounds derived from the propagation of the instrumental noise. This would add confidence to the results, for example the comparison between experimental and theoretical Stokes drift fluxes."

S2 Method

The first two sections list the general definition used to compute the propagation of uncertainty measurements.

S2.1 General statistics

We recall the definition of the variance. We use it to express the uncertainty due to filtering in section 2.6.

S2.1.1 Measured value vs. true value

We assume that the true physical quantity is denoted by X_{true}. The instrument provides a noisy measurement

$$X_{\text{mes}} = X_{\text{true}} + \delta_X \tag{S1}$$

where δ_X is the measurement error (assumed to have zero mean if the instrument is unbiased).

S2.1.2 Variance as the ensemble average of squared errors

The variance of the measurement error is defined as

$$\sigma^2 = \mathbb{E}\big[\,(X_{\text{mes}} - X_{\text{true}})^2\,\big] = \mathbb{E}\big[\delta_X^2\big], \tag{S2}$$

that is, the ensemble average of the squared differences between the measured value and the true value.

S2.2 The general propagation of uncertainty

We use the propagation of errors formula to express the error of a quantity F calculated from a combination of n variables x_i.

$$\sigma_F^2 = \left(\frac{\partial F}{\partial x_1}\right)^2 \sigma_{x_1}^2 + \left(\frac{\partial F}{\partial x_2}\right)^2 \sigma_{x_2}^2 + ... + \left(\frac{\partial F}{\partial x_N}\right)^2 \sigma_{x_N}^2 \tag{S3}$$

The propagation error formula can be used for the case of small error terms and uncorrelated, independent variables. It can be found using equation 1, more information on the formula is in section 3.16.8 in the book [Emery and Thomson 2001 - ISBN 978-0-12-387782-6].

S2.3 Total transport

The total transport is expressed as :

$$Q(t,T) =< \int_{z(T_1,t)}^{z(T_2,t)} u(z,t)\ dz > \tag{S4}$$

where $z(T_i,t)$ is the height for which $T(z,t) = Ti$ and $u(z,t)$ is the horizontal cross-shelf velocity. The temperature and the velocity are independent and collocated on a regular grid. Notation $< . >$ represents low-pass filtering.

S2.3.1 The uncertainty on unfiltered transport

The unfiltered transport is expressed as :

$$Q'(t,T) = \int_{z(T_1,t)}^{z(T_2,t)} u(z,t)\ dz \tag{S5}$$

The discrete form is :

$$Q'(t;T_1,T_2) = \delta_h \sum_{k=k_1}^{k_2} u_k(t) \tag{S6}$$

With δ_h the spacing of the vertical grid and k the vertical level index.
Applying equation S3 to equation S6 we find :

$$\sigma_{Q'}^2(t) = \delta_h^2 \sum_{k=k_0}^{k_1} \sigma_u^2 + u(z_{(T_1)},t)^2 \sigma_{z_{(T_1)}}^2 + u(z_{(T_2)},t)^2 \sigma_{z_{(T_2)}}^2 \tag{S7}$$

$$\sigma_{Q'}^2(t) = M\delta_h^2\sigma_u^2 + u(z_{(T_1)})^2 \sigma_{z_{(T_1)}}^2 + u(z_{(T_2)})^2 \sigma_{z_{(T_2)}}^2 \tag{S8}$$

Where
$M = k_2 - k_1 + 1$
σ_u is the standard deviation on one ping for a given ADCP configuration and σ_z is the uncertainty in the isotherm height. The variance $\sigma_{z(T_i)}$ is defined in the next section.

S2.4 Interpolation and filter

S2.4.1 The uncertainty in the isotherm height z(T$_i$)

The uncertainty in the isotherm height is denoted $\sigma_{z(T_i)}$. It depends on the temperature and pressure measurement noise and on the temperature interpolation. The measurements from sensors a and b are denoted (T_{ma} , z_{ma}) and (T_{mb} , z_{mb}). Between two sensor the temperature is linearly interpolated. The interpolated temperature field is denoted Ti and expressed as :

$$T_i = (z - z_a)\frac{T_b - T_a}{z_b - z_a} + T_a \tag{S9}$$

We define $H = z_b - z_a,\ D = T_b - T_a,\ N = T_i - T_a$, so that :

$$z(T_i) = z_a + H\frac{N}{D} \tag{S10}$$

The variance is computed using equation S3 and we note $\sigma_{T_a} = \sigma_{T_b} = \sigma_{T_m}$ and $\sigma_{z_a} = \sigma_{z_b} = \sigma_{z_m}$.

$$\sigma_{z(T_i)}^2 = \sigma_{T_m}^2\big((\tfrac{z_b-z_a}{(T_b-T_a)^2}(T_a - T_i))^2 + (\tfrac{z_b-z_a}{(T_b-T_a)^2}(Ti - Tb))^2\big) + \sigma_{z_m}^2\big((\frac{T_i - T_a}{T_b - T_a})^2 + (1 - \frac{T_i - T_b}{T_b - Ta})^2\big) \tag{S11}$$

and using the expression defined above we can write :

$$\sigma_{z(T_i)}^2 = \sigma_{T_m}^2 \frac{H^2}{D^4}((N-D)^2 + N^2) + \sigma_{z_m}^2\big((1-\tfrac{N}{D})^2 + (\tfrac{N}{D})^2\big) \tag{S12}$$

The contribution of σ_{T_m} increases when the distance between the two measurement points increases, and when D decreases, i.e when the two measurements are similar. The contribution of σ_{z_m} is bounded by a multiplication factor 0.5 when $T_i = \frac{Tb+Ta}{2}$ and 1, when $T_i = T_a$ or $T_i = T_b$. Therefore, the main source of error in the isotherm height is expected to be the temperature measurement. This error is reduced when the sensors are close to each other but distant enough to measure distinct temperature.

S2.4.2 The uncertainty due to filtering

The filter used is a Butterworth low-pass filter of order 3 from scipy.signal python package. We applied it to a time series with a sampling frequency fs which depends on the data set (N-BoB or SE-BoB) and a cut-off frequency f_c of 1/(24 hours). The filters impulse response is denoted $h(t)$ (see Figure S1) and is applied forward and backward using scipy.signal.filtfilt().

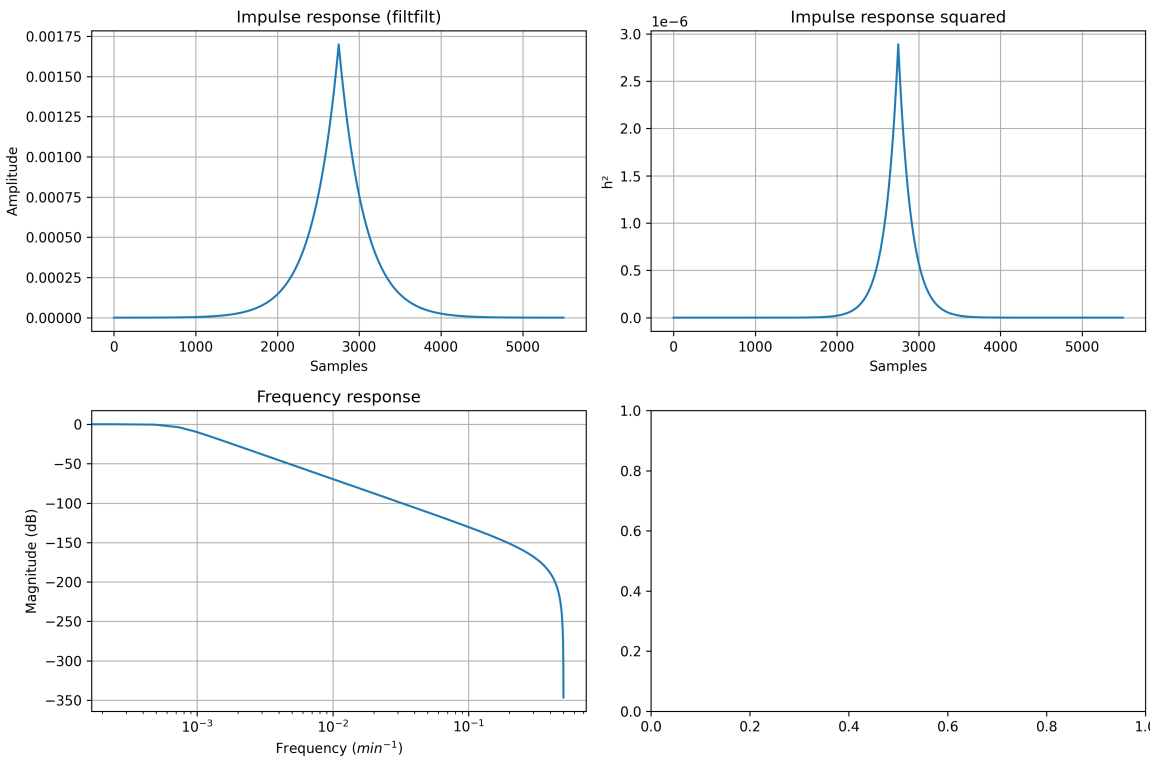

Figure S1: Characteristics of the Butterworth low pass filter of 3rd order used on SE-BoB dataset : the cut-off frequency is $f_c = 1/(24.60)$ and the frequency sampling is $fs = 1$.

We denote the unfiltered transport Q' and $\delta_{Q'}$ the measurement error. The error is non stationary.

$$Q(t) = h * Q'(t) = \int_{-\infty}^{\infty} h(\tau)Q'(t-\tau)d\tau \tag{S13}$$

Using the measured value vs. true value concept described in section 2.1.1 it can be shown that :

$$\begin{aligned}
\delta_Q(t) &= \int_{-\infty}^{\infty} h(\tau)\delta_{Q'}(t-\tau)d\tau \\
\mathbb{E}[\delta_Q^2(t)] &= \iint_{-\infty}^{\infty} h(\tau)h(\tau')\mathbb{E}[\delta_{Q'}(t-\tau)\delta_{Q'}(t-\tau')]d\tau d\tau'
\end{aligned}$$

Where $\mathbb{E}$ is the ensemble average. We assume the errors to be δ-correlated so that :

$$\mathbb{E}[\delta Q(t-\tau)\delta Q(t-\tau')] = \sigma_{Q'}^2(t-\tau)\delta(\tau-\tau')$$

Where $\delta(t)$ is the Dirac function and therefore :

$$\sigma_Q^2 = \iint_{-\infty}^{\infty} h(\tau)h(\tau')\sigma_{Q'}^2(t-\tau)\delta(\tau-\tau')d\tau d\tau' \tag{S14}$$

$$\sigma_Q^2 = \int_{-\infty}^{\infty} h^2(\tau)\sigma_{Q'}^2(t-\tau)d\tau \tag{S15}$$

The variance σ_Q^2 is obtained by filtering the variance of the unfiltered transport $\sigma_{Q'}^2$ using the squared impulse response of the filter (see Figure S1).

S2.5 Eulerian transport

Eulerian transport is computed using the filtered velocity $< u(z,t) >$ and the filtered temperature field. The height of the filtered isotherm is denoted $z_{Eu}(T,t)$. We can write the Eulerian transport as :

$$Q_{Eu}(t,T) = \int_{z_{Eu}(T_1,t)}^{z_{Eu}(T_2,t)} < u(z,t) > dz \tag{S16}$$

Using equation S3 we can write the uncertainty in Eulerian transport as :

$$\sigma^2_{Q_{Eu}}(t,T) = M\delta_h^2 \sigma_{<u>}{}^2 + < u(z_{Eu(T_1)}) >^2 \sigma^2_{z_{Eu(T_1)}} + < u(z_{Eu(T_2)}) >^2 \sigma^2_{z_{Eu(T_2)}} \tag{S17}$$

where M and δh definitions are given in section 2.3. With the uncertainty due to filtering expressed in section 2.4.2 we can write :

$$\sigma^2_{<u>} = \int_{-\infty}^{\infty} h^2(\tau)\sigma_u^2(t-\tau)d\tau \tag{S18}$$

$$\sigma^2_{z_{Eu}} = \int_{-\infty}^{\infty} h^2(\tau)\sigma_z^2(t-\tau)d\tau \tag{S19}$$

S2.6 Residual transport

Residual transport is the difference between Eulerian and total transport. We masked the residual transport when the Eulerian and total transport were uncertain (error up to 50 % of the value).

S3 Results

S3.1 Total transport

We present the uncertainty on transport for the SE-BoB dataset. Equivalent work could be done on the N-BoB dataset. At the SE-BoB $\sigma_u = 0.08\ m/s$, $\sigma_{Tm} = 0.1\ °C$ and $\sigma_{zm} = 0.1\ m$.

S3.1.1 Error contribution before filtering

We identify which term contributes the most to the uncertainty in equation S8, between σ_u and $\sigma_{z(T_i)}$ (Figure S2). The velocity error dominates near the boundary, where the temperature is the measured temperature. In the interior, the Temperature/Pressure error dominates most of the time due to the distance between the sensors (H=10 m in SE-BoB dataset). At high frequency, the velocity error can dominate (Figure S2). The velocity error dominates regularly at the same temperature range. This is likely due to an isotherm that regularly matched one of the temperature sensors and was likely close to a strongly stratified location. The values are set to NaN when no transport is measured or it is smaller than the error. To apply the filter we filled the variance time series with it's time average.

The maximum variance of the total transport after the 24h low pass filter is 0.035 m^2/s (Figure S3). The maximum values are between 16 and 20 $°C$ before 17th July, when the transport reached a maximum of $-1.4\ m^2/s$ (Figure S4).

S3.1.2 Total transport time series and profile

Where the variance reached more than 50% of the transport we masked the transport (Figure S4). The main structures were not masked.

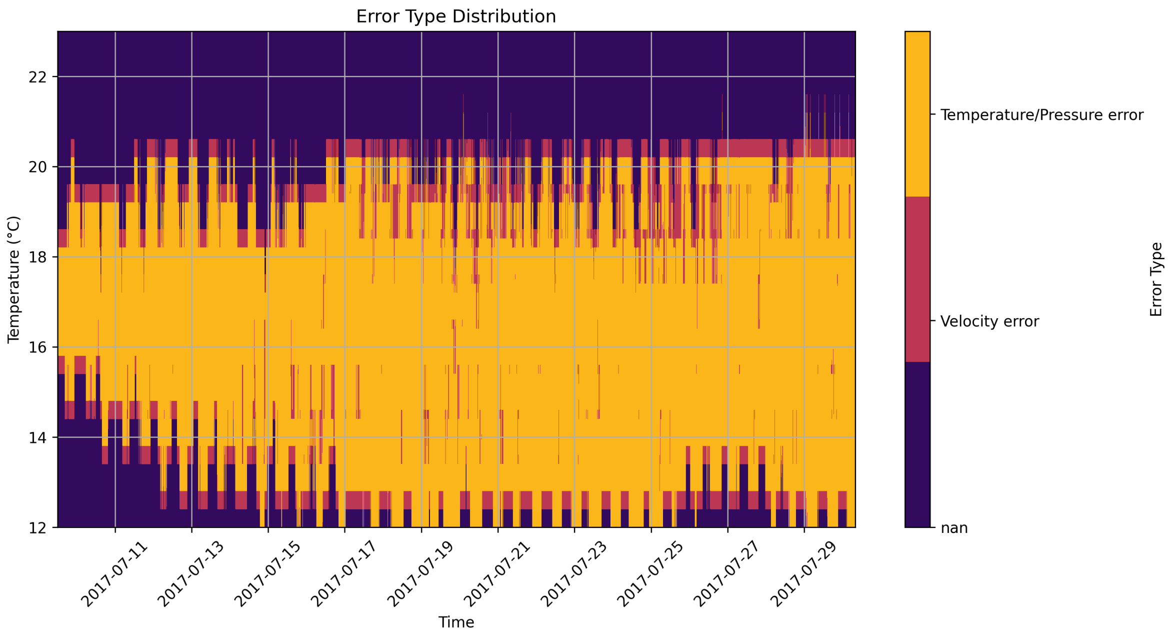

Figure S2: Error type at each time step and each temperature range from equation S8.

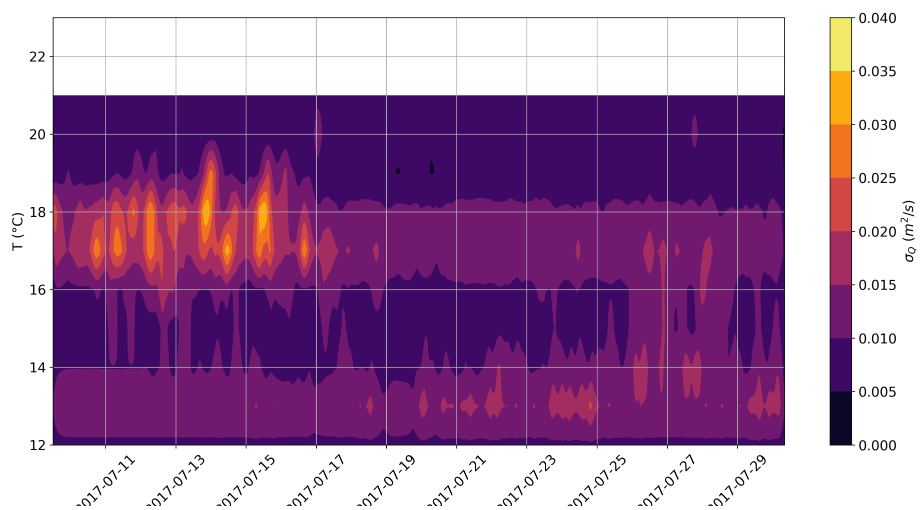

Figure S3: The variance on total transport σ_Q due to the propagation of the measurement uncertainties

S3.2 Eulerian transport variance and mask

The variance was smaller for Eulerian transport than total transport. The maximum variance on Eulerian transport was $0.008m/s$ (Figure S5). For ease of computation $\sigma_{z_{Eu}}$ was computed using a constant $\sigma_z = 0.7m$, obtained from equation S12 with $H = 10m$, $D = 1°C$ and $N = 0.5°C$. These values were chosen from the average temperature profile and sensor position shown in Figure 1 of the manuscript. Due to the filter, uncertainty was reduced: $\sigma_{z_{Eu}} = 0.02m$.

We masked the transport where the variance reached more than 50% of the transport (Figure S6). Almost no data were masked on the Eulerian field.

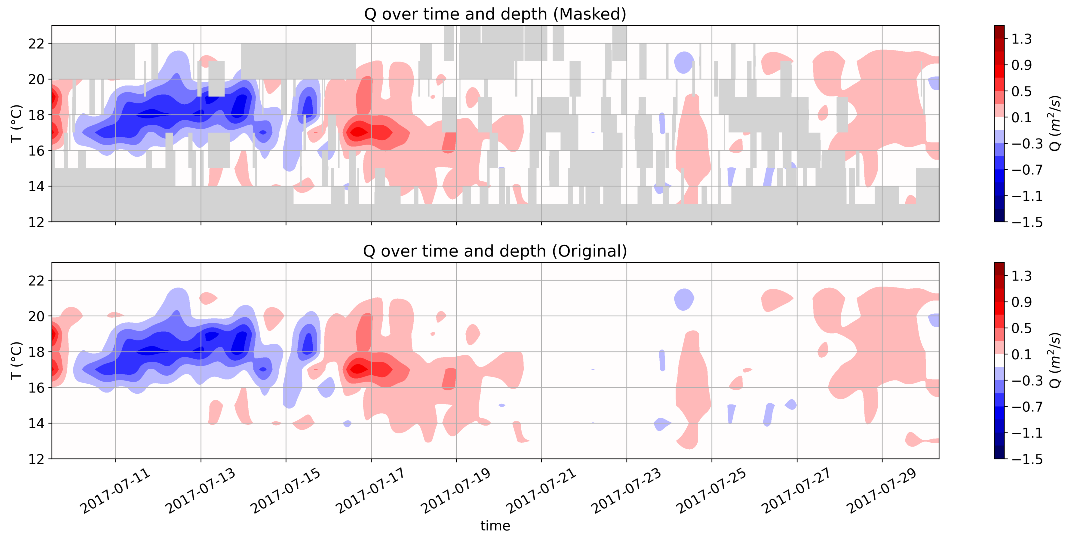

Figure S4: (Top) Total transport masked when the error is more than 50 % of the value (bottom) Original transport

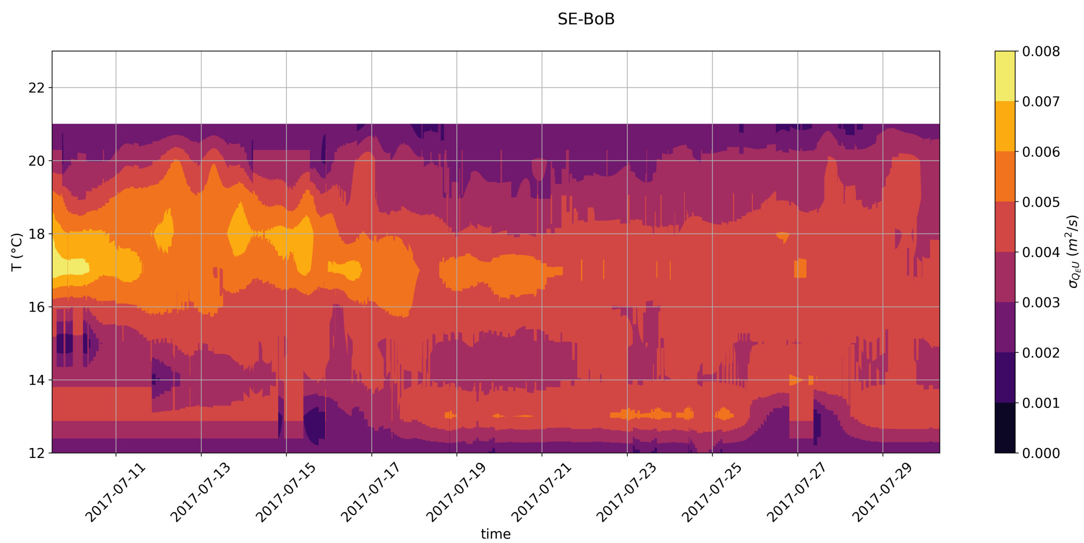

Figure S5: Variance on Eulerian transport as a function of time and temperature range. For the SE-BoB site.

S3.2.1 Residual transport time series and vertical profile

The variance in residual transport was dominated by the variance on total transport. Based on Figure S3 the variance in residual transport was of the same order : 10^{-2} m^2/s.

We applied the two masks from the total transport and Eulerian transport analyses to residual transport (Figure S7). Positive transport near the bottom (where the temperature is below 14 °C) was partly masked.

The time average was affected by the mask mostly for temperatures below 14°C (Figure S8 and S9). Where the transport was NaN we considered the transport to be nil as initial values were all close to zero. The positive transport for low temperature remained positive but was reduced between the original and masked transport.

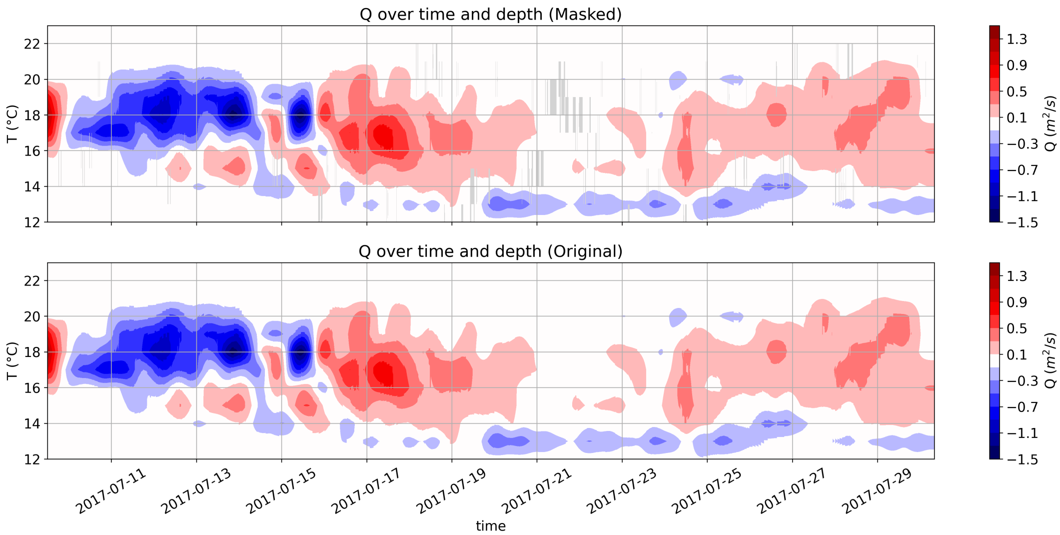

Figure S6: (Top) Eulerian transport masked when the error is more than 50 % of the value. (bottom) Original Eulerian transport

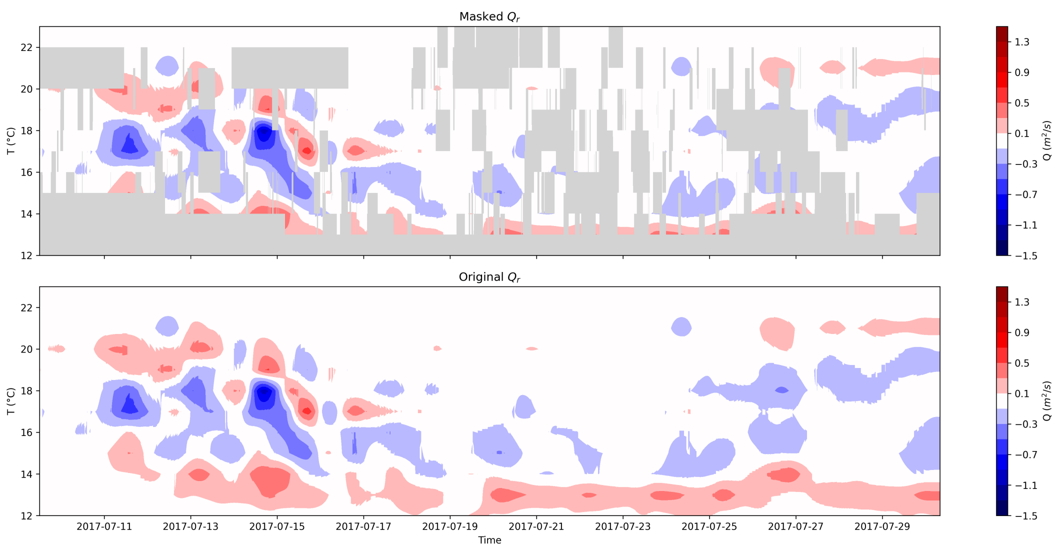

Figure S7: (Top) Residual transport masked with the combined mask from total and Eulerian analysis. (bottom) Original residual transport

S4 Conclusion and acknowledgement

Most of the variance in the measurements was due to temperature. The main source of uncertainty in residual transport was the uncertainty in total transport. Masking the value did not remove the main structures observed and described in the paper. The vertical profile of residual transport remained unchanged. The analysis confirmed the results observed in the manuscript.

We would like to express our sincere gratitude to Louis Marié (Ifremer LOPS) for his invaluable assistance in addressing the impact of filters on uncertainty. We also acknowledge the use of the GPT-4o model in developing the code.

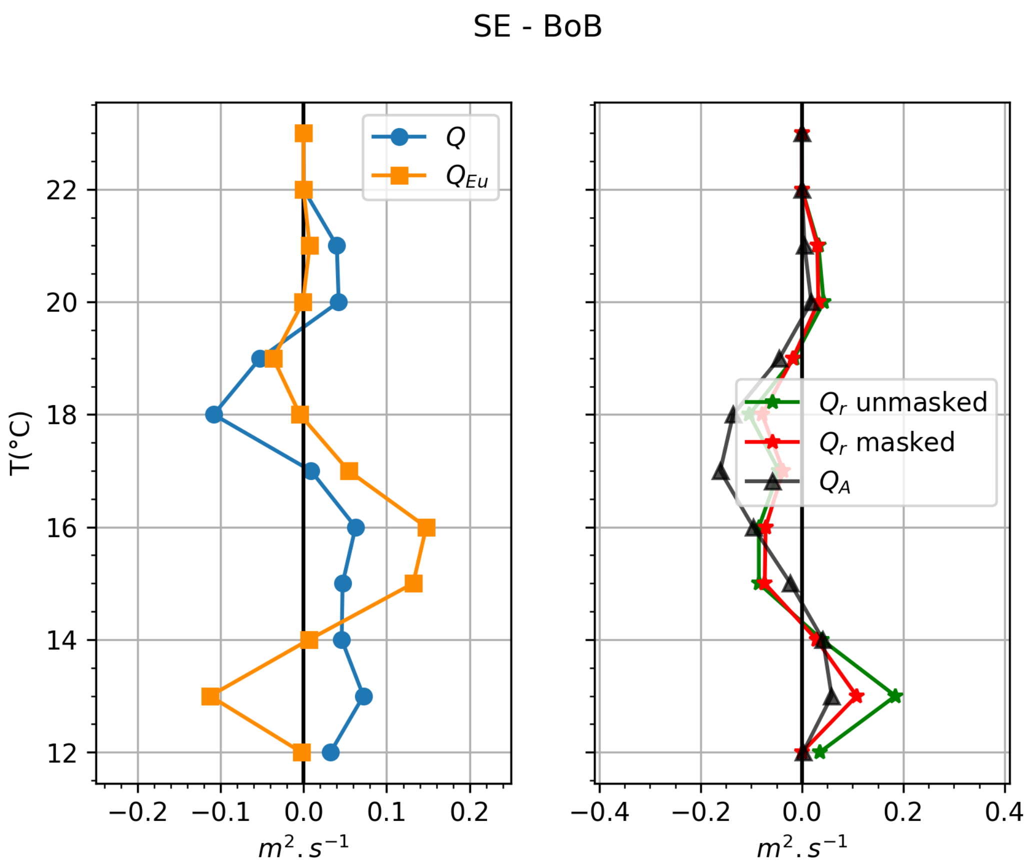

Figure S8: Vertical profile of original residual transport (black) and masked residual transport (red) averaged on the total time series

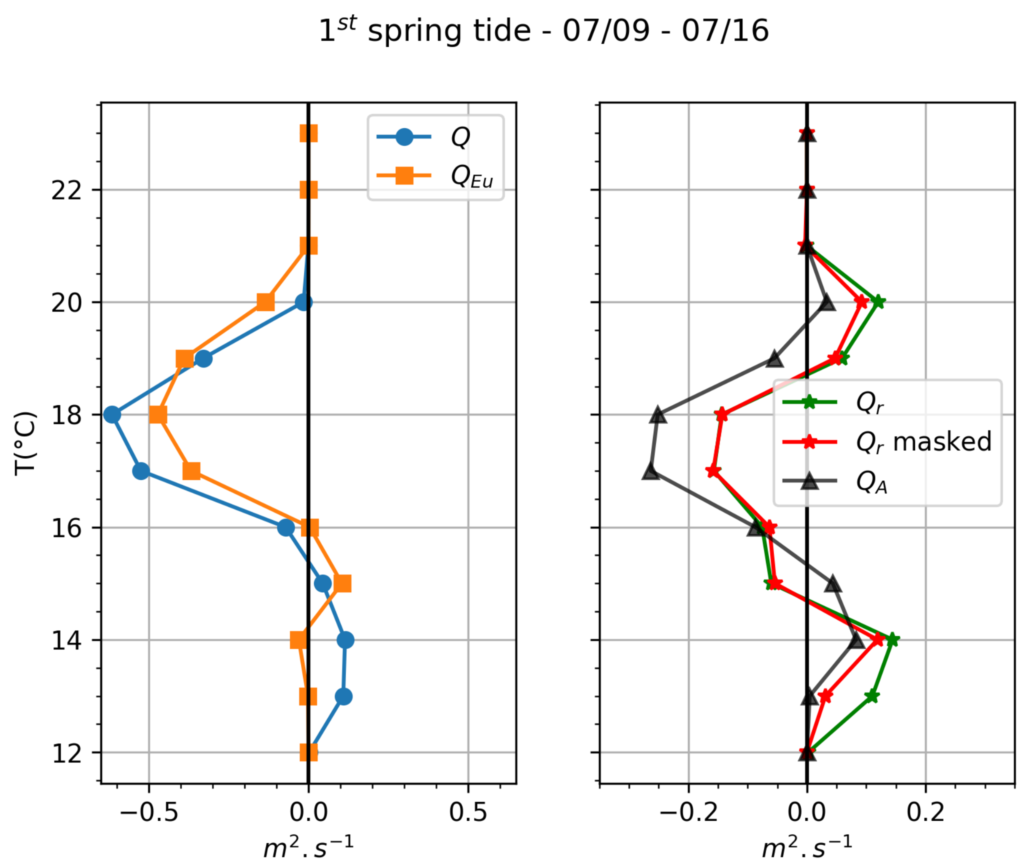

Figure S9: Vertical profile of original residual transport (black) and masked residual transport (red) averaged on the 1st spring tide

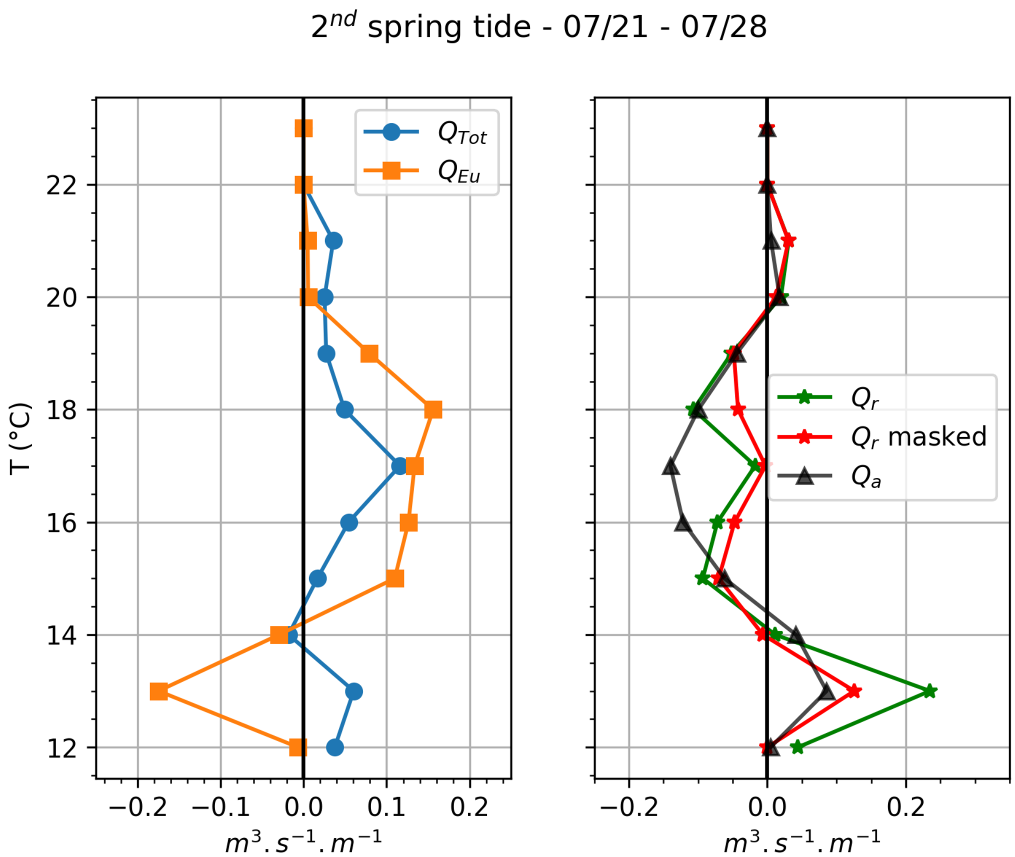

Figure S10: Vertical profile of original residual transport (black) and masked residual transport (red) averaged on the 1st spring tide